

ARO 17687.4-EL-A

JOURNAL DE PHYSIQUE

Colloque C7, supplément au n°10, Tome 42, octobre 1981

page C7-63

(2)

BAND-STRUCTURE DEPENDENT IMPACT IONIZATION IN SILICON AND GALLIUM ARSENIDE

J.Y. Tang, H. Shichijo, K. Hess and G.J. Iafrate\*

Coordinated Science Laboratory and Department of Electrical Engineering, University of Illinois at Urbana-Champaign, Urbana, Illinois, U.S.A. 61801

\*U.S. Army Electronics Technology and Device Laboratory, Ft. Monmouth, New Jersey U.S.A. 07703

**Résumé.** - Nous avons développé une simulation par la méthode de Monte Carlo pour du silicium et de l'AsGa en incluant une structure de bande réaliste. Les taux d'ionisation par impact et les vitesses de dérive en régime continu sous forts champs électriques ( $> 100$  kV/cm) ont été calculés à différentes températures.

**Abstract.** - We have performed a Monte Carlo simulation for GaAs and Si with the realistic band structure included. Steady state impact ionization rates and drift velocities under high electric fields ( $> 100$  kV/cm) were calculated at various temperatures.

1. **Introduction.** - Impact ionization is an essential mechanism in the operation of semiconductor devices such as avalanche photo-diodes or transit time devices. The dependence of impact ionization on the crystallographic orientation has attracted substantial interest because of its relevance to noise and other phenomena in these devices. This dependence, however, is not shown by any of the theories as given by Wolff [1], Shockley [2], and Baraff [3], since none of them include a realistic band structure.

We have developed a complete theory for impact ionization and generally high field transport in semiconductors by combining a Monte Carlo simulation with the realistic band structure calculated by the empirical pseudopotential method. We do take into account scattering by all possible phonon types, the change in the density of states high in the band, the exact velocity  $\vec{v} = \frac{1}{\hbar} \vec{v}_k E(\vec{k})$  (no effective mass approximation), the collision broadening of the electronic states, and the temperature effect.

Details of the model and the results for GaAs at 300 K can be found in two of our previous papers [4,5]. In the case of Si, the first two conduction bands were included. Besides the X-X scattering we also include the X-L scattering in Si. In Section 2, we describe briefly our model and point out its differences from the commonly used model. The effects of the inclusions of the second band and the transition from X-L in Si are discussed in Section 4.

2. **Theoretical Model.** - The model for Monte Carlo simulation has two main ingredients: (i) the band structure and (ii) the scattering rate. We describe briefly in the following the different features that have been included in our model and the advantages it has over other models.

AD A116011

FILE COPY

DMS

82 06 21 008

2.1. Band Structure - Instead of using a parabolic band approximation, we incorporated into this Monte Carlo simulation a realistic band structure calculated by the empirical pseudopotential method [6] for both GaAs and Si. The realistic band structure enables us to carry out the simulation up to very high electric fields without worrying about the breakdown of a constant mass approximation which is usually adopted. The first two conduction bands are included for Si. Only the first conduction band is included for GaAs because the second band lies significantly higher up.

2.2. Scattering Rate -

(i) GaAs: Polar optical scattering and equivalent and nonequivalent intervalley scattering were included in the model. We did not include impurity scattering and acoustic phonon scattering whose effect are small compared to other scattering mechanisms. The reader should refer to our previous paper for more details and numerical parameters [4].

(ii) Si: We followed closely the work by Canali et al.[7-9] in the case of Si. For simplification, the intravalley acoustic phonon scattering was considered elastic, which is good for the high field region we were interested in. The nonparabolicity factor was also included [9]. For X-X coupling we considered several possible phonon types (3f and 3g). The difference between f and g scattering was taken into account in the simulation process.

Besides the equivalent (X-X) intervalley scattering, we also included the nonequivalent (X-L) intervalley scattering mechanism. The X-L coupling constants were assumed to be the same for all four possible phonons determined from the phonon spectrum [10] and were found to be  $3.5 \times 10^8$  eV/cm by fitting the calculated results to the experimental results.

The longitudinal and transverse effective masses of the L-valley were determined from the pseudopotential band structure to be  $m_L = 1.59 m_0$  and  $m_t = 0.121 m_0$ . The L-valleys lie about 1 eV above the X-valleys. The effect of the L-valleys is important only at high fields ( $> 100$  kV/cm).

(iii) Scattering rate at high energy: The effective mass density of states with the nonparabolicity factor included was used in calculating the scattering rates. It is not appropriate to simply extend these scattering rates to higher energies because the effective mass approximation breaks down at higher energies and the density of states starts decreasing at some critical point. The intervalley scattering rate, which is proportional to the final density of states, should be modified at higher electron energies. Therefore we have calculated the total density of states for one conduction band for GaAs and two conduction bands for Si. The critical points beyond which the density of states decreases for GaAs and Si were found to be 1.8 eV and 2 eV, respectively. The density of states decreases almost quadratically above that. We therefore have assumed a quadratic decrease of the scattering rates above the critical points.

(iv) Scattering probability for impact ionization: Impact ionization can be treated as an additional scattering mechanism. We assume an isotropic threshold energy for both GaAs (2.0 eV) and Si (1.8 eV) [12]. The formula for the probability of impact ionization above threshold can be found in a paper by Keldysh [11].

2.3. Temperature Effect - We assumed that the band structure is essentially unaltered with changes in temperature except that the band gap is modified. We further assumed that the threshold energy of impact ionization can be scaled according to the formula

$$E_{th}(T) = \frac{E_g(T)}{E_g(300K)} \cdot E_{th}(300K).$$

The formula for the temperature dependence of the band gap  $E_g$  can be found in [19] both for Si and GaAs.

2.4. Collision Broadening Effect - As the scattering rate goes up to  $10^{14}$  per second, the energy of the electron is uncertain within  $\Delta E \sim \hbar/\tau$  according to uncertainty principle.  $\Delta E$  is about 100 meV for  $1/\tau$  higher than  $10^{14}$ . In determining the final state after each scattering, we considered the states within a range  $\Delta E$  of the true final state energy as possible candidates. We then chose randomly one of those candidates as the final state, keeping the average energy loss (gain) constant. The collision broadening effect should be taken into account automatically by so doing.

### 3. Results

3.1. GaAs: Figure 1 shows the electron ionization rate  $\alpha$  at two temperatures. The result for 300 K was shown in a previous paper [4] and the shaded region is the range covered by available experimental results for 300 K. The experimental result for 77 K is not available at this time. The lower temperature of 77 K should result in a higher impact ionization rate as shown in the graph. As we have discussed in the previous paper, our calculations showed no orientational dependence for fields higher than 300 kV/cm.

3.2. Si: We have calculated drift velocities in the <111> direction for high electric fields and compared them to the recent high field experimental results by Smith et al. [20]. As shown in Figure 2, our calculated high field results are in good agreement with the experimental results. In Figure 3 we show the calculated results of the electron impact ionization rate  $\alpha$  at two temperatures, 100 K and 300 K. For 300 K our results seem to agree better with Lee and Logan's results than with Overstraeten and De Man's results. Again, like in GaAs, we did not find any orientational dependent ionization rate in Si. As we mentioned in Section 2 of this paper, the first two conduction bands were included in the model. We show an interesting but important result in Figure 4 which tells us the important role played by the second conduction band in the transport of electrons in Si. We plotted on the graph both the second band effect and the average energy of electrons as a function of electric field. From the pseudopotential band structure, the

minima of the second conduction band are located exactly at X. They are about 0.1 eV above the minima of the first conduction band. The electrons can be scattered to the second band once their energies get above 0.1 eV. The correlation between the second band effect and average electron energy shows clearly in the graph. The decrease of the effect of the second band after 100 kV/cm is probably because of the slower relative increase of the density of states of the second band compared to the first band.

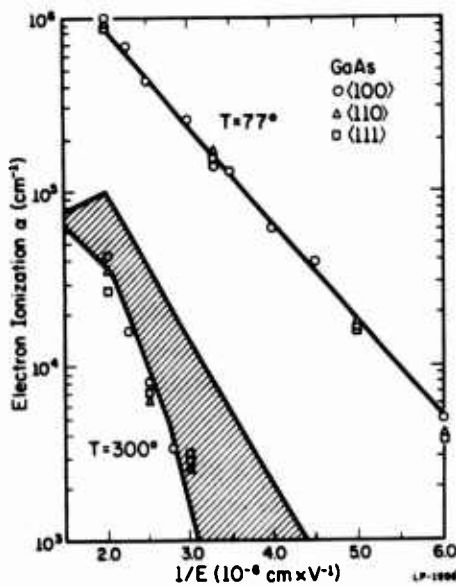


Fig. 1: Results of calculated impact ionization rate  $\alpha$  for GaAs at two different temperatures, 77 K and 300 K, plotted as a function of inverse electric field. The shaded region is the range covered by available experimental results [15-18].

Erratum.—A correction needs to be made to figure (1), the electron ionization rate vs.  $1/E$ . The curve for  $T = 77$  K corresponds to the scale on the right hand side. Inadvertently the labels on the right hand side were omitted. These were a factor of ten lower than those corresponding to the left hand side in order to avoid clutter in the diagram. The text, conclusions, and other diagrams remain valid.

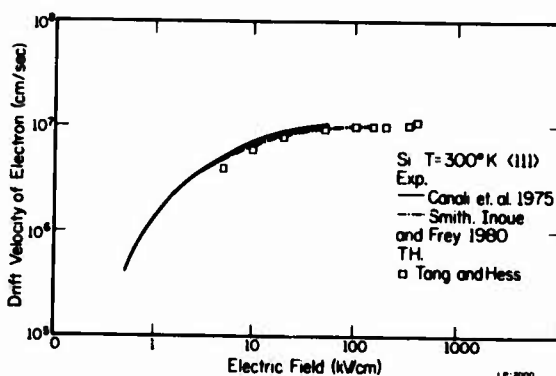


Fig. 2: Calculated drift velocity of Si in <111> direction. The solid line and the dashed line are the experimental results of Canali et al. and Smith et al., respectively.

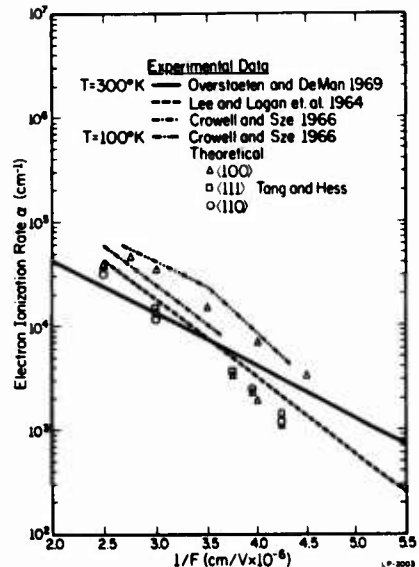


Fig. 3: Calculated impact ionization rate  $\alpha$  at two different temperatures in Si plotted as a function of inverse electric field. For  $T = 300$  K, we calculated the ionization rate  $\alpha$  in three different crystallographic directions. Only  $<100>$  directions were calculated for 100 K. The lines are the experimental results from different authors [12-14].

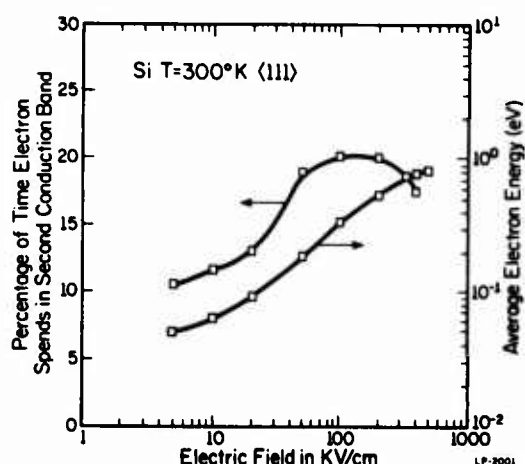


Fig. 4: We plotted the second band effect and the average energy of electrons as a function of electric field. The left scale corresponds to the upper curve and the right scale corresponds to the lower curve.

#### 4. Discussion

4.1. GaAs: The transport properties of GaAs were discussed in detail in our previous papers [4,5]. From the present 77 K result for the impact ionization rate  $\alpha$ , we see again that no orientational dependence was found. From the drift velocity results [4], it appears that modification of the coupling constants is needed for a realistic band structure. A better fit to the experimental data should result from the modification of the coupling constants.

4.2. Si: As can be seen from Fig. 4, the second band effect is of significance to the transport of electrons in Si. Previous Monte Carlo Calculations by the Italian group [7-9] produced a drift velocity consistently higher than the experimental values. We believe the reason for this lies in the neglect of the second band which enhances the scattering rate of electrons for energies above 0.1 eV. The scattering percentage due to X-L scattering, as seen from our simulation, is significant only when the electric field is above 100 kV/cm. The drift velocity for electric fields under 100 kV/cm is basically not influenced by adjusting the X-L coupling constant. The impact ionization rate is very sensitive to this coupling constant because X-L scattering is significant when the electric field is above 200 kV/cm. For an assumed isotropic threshold energy in Si of 1.8 eV [12], a coupling constant of  $3.5 \times 10^8$  eV/cm is obtained by fitting the experimental data at 333 kV/cm. In a recent paper by Thornber [21] a threshold energy of 3.6 eV was obtained from fits to the experimental data. (The paper contains simplifying assumptions.) We have tried to adjust the values of the X-L coupling constant and the threshold energy of ionization to see if such a high threshold is possible. We found that a threshold energy of 2.4 eV is needed to fit the experimental data at 333 kV/cm if we completely neglect the X-L coupling effect. A threshold of 3.6 eV seems therefore too high.

Acknowledgements. - The authors wish to thank K. F. Brennan for help in the computer work and G. E. Stillman for many valuable discussions. The use of the computer facilities of the Materials Research Laboratory, University of Illinois, is also gratefully acknowledged. This work was supported by the Office of Naval Research, the Army Research Office, and the Joint Services Electronics Program.

#### References

1. P. A. Wolff, Phys. Rev. 95, 1415 (1954).
2. W. Shockley, Solid State Electron. 2, 35 (1961).
3. G. A. Baraff, Phys. Rev. 128, 2507 (1962).
4. H. Shichijo and K. Hess, Phys. Rev. B, 23, 4197 (1981).
5. H. Shichijo, K. Hess and G. E. Stillman, Appl. Phys. Lett. 38, 89 (1981).
6. M. L. Cohen and T. K. Bergstresser, Phys. Rev. 141, 789 (1966).
7. C. Canali, C. Jacoboni, F. Nava, G. Ottaviani, and A. Alberigi-Quaranta, Phys. Rev. B 12, 2265 (1975).
8. C. Jacoboni, C. Canali, G. Ottaviani and A. Alberigi-Quaranta, Solid-State Electron. 20, 77 (1977).
9. C. Jacoboni, R. Minder and G. Majni, Phys. Chem. Solidi 36, 1129 (1975).
10. D. Long, Phys. Rev. 120, 2024 (1960).
11. L. V. Keldysh, Sov. Phys. JETP 21, 1135 (1965).
12. R. Van Overstraeten and H. De Man, Solid State Electron 13, 583 (1970).
13. C. R. Crowell and S. M. Sze, Appl. Phys. Lett. 9, 242 (1966).
14. C. A. Lee, R. A. Logan, R. L. Bardorf, J. J. Kleimack, and W. Wiegmann, Phys. Rev. 134, A761 (1964).

15. S. N. Shadbe and C. Yeh, *J. Appl. Phys.* 41, 471 (1974).
16. G. E. Stillman, C. M. Wolfe, J. A. Rossi, and A. G. Foyt, *Appl. Phys. Lett.* 24, 471 (1974).
17. H. D. Law and C. A. Lee, *Solid-State Electron.* 21, 331 (1978).
18. T. P. Pearsall, F. Capasso, R. E. Nabory, M. A. Pollack, and J. R. Chelikowsky, *Solid-State Electron.* 21, 297 (1978).
19. J. I. Pankove, Optical Process in Semiconductors, Dover Publications, Inc.
20. P. M. Smith, M. Inoue, and J. Frey, *Appl. Phys. Lett.* 37, 797 (1980).
21. K. K. Thornber, *J. Appl. Phys.* 52, 279 (1981).

REPORT DOCUMENTATION PAGE		READ INSTRUCTIONS BEFORE COMPLETING FORM
1. REPORT NUMBER  17687.4-EL-A	2. GOVT ACCESSION NO.  A71A11601	3. RECIPIENT'S CATALOG NUMBER  N/A
4. TITLE (and Subtitle)  Band-Structure Dependent Impact Ionization in Silicon and Gallium Arsenide	5. TYPE OF REPORT & PERIOD COVERED  Reprint	
	6. PERFORMING ORG. REPORT NUMBER  N/A	
7. AUTHOR(s)  J. Y. Tang, H. Shichijo, K. Hess, G. J. Iafrate	8. CONTRACT OR GRANT NUMBER(s)  DAAG29 80 K 0069	
9. PERFORMING ORGANIZATION NAME AND ADDRESS  University of Illinois Urbana, IL 61801	10. PROGRAM ELEMENT, PROJECT, TASK AREA & WORK UNIT NUMBERS  N/A	
11. CONTROLLING OFFICE NAME AND ADDRESS  U. S. Army Research Office P. O. Box 12211 Research Triangle Park, NC 27709	12. REPORT DATE  Oct 81	
14. MONITORING AGENCY NAME & ADDRESS (if different from Controlling Office)	13. NUMBER OF PAGES  7	
	15. SECURITY CLASS. (of this report)  Unclassified	
	15a. DECLASSIFICATION/DOWNGRADING SCHEDULE	
16. DISTRIBUTION STATEMENT (of this Report)  Submitted for announcement only.	Accession For  NTIS GRA&I DTIC TAB Unannounced <input type="checkbox"/> Justification  By _____ Distribution/ Availability Codes Avail Author Dist Special	
17. DISTRIBUTION STATEMENT (of the abstract entered in Block 20, if different from Report)		
18. SUPPLEMENTARY NOTES	DTIC COPY INSPECTED 2	
19. KEY WORDS (Continue on reverse side if necessary and identify by block number)	A71	
20. ABSTRACT (Continue on reverse side if necessary and identify by block number)	DTIC REF ID: A71 JUN 23 1982 H	